

Ultrasound, eddy current and magnetic Barkhausen noise as tools for sigma phase detection on a UNS S31803 duplex stainless steel

Paulo G. Normando^a, Elineudo P. Moura^{a,*}, José A. Souza^b, Sérgio S.M. Tavares^b, Linilson R. Padovese^c

^a Universidade Federal do Ceará, Department of Metallurgical and Materials Engineering, Campus do Pici, Bloco 714, CEP 60455-760, Fortaleza, CE, Brazil

^b Universidade Federal Fluminense, Department of Mechanical Engineering, Rua Passo da Pátria, 156, CEP 24210-240, Niterói, RJ, Brazil

^c Universidade de São Paulo, Department of Mechanical Engineering, CEP 05508-900, São Paulo, SP, Brazil

ARTICLE INFO

Article history:

Received 21 August 2009

Received in revised form 1 January 2010

Accepted 6 January 2010

Keywords:

Duplex steel

Heat treatment

Phase transformation

Nondestructive testing

ABSTRACT

Sigma phase is a deleterious one which can be formed in duplex stainless steels during heat treatment or welding. Aiming to accompany this transformation, ferrite and sigma percentage and hardness were measured on samples of a UNS S31803 duplex stainless steel submitted to heat treatment. These results were compared to measurements obtained from ultrasound and eddy current techniques, i.e., velocity and impedance, respectively. Additionally, backscattered signals produced by wave propagation were acquired during ultrasonic inspection as well as magnetic Barkhausen noise during magnetic inspection. Both signal types were processed via a combination of detrended-fluctuation analysis (DFA) and principal component analysis (PCA). The techniques used were proven to be sensitive to changes in samples related to sigma phase formation due to heat treatment. Furthermore, there is an advantage using these methods since they are nondestructive.

© 2010 Elsevier B.V. All rights reserved.

1. Introduction

Duplex stainless steels (DSS) are corrosion resistant materials which are advantageous by presenting a higher mechanical strength than conventional austenitic (300 series) and ferritic stainless steels. The Cr, Mo and N additions increase the pitting corrosion resistance to a level superior to the one for AISI 316L and 317L steels while almost doubling yield strength [1]. However, duplex steels are susceptible to formation of deleterious phases during high temperature processing such as hot forming, heat treatment and welding. In duplex steel UNS S31803, sigma phase (σ) and other deleterious phases such as chi (χ) and secondary austenite form from ferrite phase in the 600–1000 °C range [2]. In the work of Pohl et al. [3] the precipitation of σ was found to be preceded by χ during aging at 750 °C and 850 °C. These two phases cannot be distinguished by conventional metallography using light microscopy [2]. Secondary austenite (γ_2) can also precipitate with σ by an eutectoid reaction $\delta \rightarrow \sigma + \gamma_2$ [4]. A good separation between these three phases can be obtained by backscattered electron imagery in a scanning electron microscope [2,4] which is a destructive method. The fact is that σ and χ phases are very detrimental to mechanical and corrosion resistance properties.

The nondestructive detection during initial stages of deleterious phases precipitation in duplex stainless steels is a challenge of great possible applications in many industrial fields.

Nondestructive testing is widely applied to detect discontinuities embedded in materials. Materials characterization is another possible application for these techniques. Each method has its advantages and drawbacks and their choice relies on the desired approach [5,6]. The objective of this work was to present an innovative approach by employing three nondestructive methods that are promising in detecting and quantifying sigma phase precipitation. The techniques were tested in a DSS UNS S31803 isothermally aged to produce different amounts of σ phase. Conventional metallography was used to quantify the deleterious phases formed. An electrolytic etching in 10% KOH solution reveals deleterious phases as dark regions leaving austenite and ferrite almost unetched [7]. Since σ forms in a much higher amount than χ and conventional light microscopy is not able to separate these two phases, it was considered that the dark regions were all correspondent to σ phase. This simple reasoning is acceptable in a practical approach because the effects of σ and χ phases on mechanical properties and corrosion resistance are very similar.

For pulse-echo ultrasonic inspection technique, a transducer of normal incidence is employed as emitter and receiver. When ultrasonic waves traveling through one medium impinge another one with significant difference in acoustic impedance like between air and metals, it will be reflected [5,6]. This is the basis for ultrasonic inspection.

* Corresponding author. Tel.: +55 85 3366 9077; fax: +55 85 3366 9969.

E-mail addresses: paulo.garcia@metalmat.ufc.br (P.G. Normando), elineudo@metalmat.ufc.br (E.P. Moura), jasouza@inpi.gov.br (J.A. Souza), ssmtavares@terra.com.br (S.S.M. Tavares), lrpadove@usp.br (L.R. Padovese).

During eddy current testing, an alternating current flows through a coil and generates a magnetic field. When this coil is brought near a conductive material, an eddy current is induced. These induced currents produce their own magnetic field (secondary) which oppose the primary field and the net effect is a weaker magnetic field that produces inductance. By measuring changes in resistance and inductive reactance of the coil, information can be gathered about the test material. This method is sensitive to changes in electrical resistivity and magnetic permeability of materials which reflect changes in chemical composition, hardness, mechanical strength, level of cold work, etc. So this method is an indirect measure of overall physical and chemical properties. Since the inductive reactance is out of phase with the resistance, vector addition must be used to calculate impedance [5,6]. This method is expected to be sensitive to sigma phase formation in duplex stainless steels.

Another nondestructive method is based on the Barkhausen effect. The Barkhausen effect refers to abrupt changes in the orientation and size of magnetic domains that occur when a moving magnetic field is applied to a ferromagnetic material. If a conducting coil is brought near a sample while a domain wall moves, an electrical pulse is produced in the coil due to the resulting change in magnetization. The detected signal is a burst of noiselike pulses called Barkhausen noise [5,6]. Domain wall motion itself is determined by many factors like microstructure, grain boundaries, inclusions, stress and strain levels [5,6].

Magnetic Barkhausen noise is nonstationary and nonlinear. However, most of the time-series analysis techniques are based on the evaluation of the properties of stationary signals [8]. Again, many conventional data analysis methods are linear. The principal component analysis (PCA) is an example of linear method [9] and for this reason it is inadequate to nonlinear data processing. On the other hand, the detrended-fluctuation analysis has shown to be adequate for analyses time series with nonlinearities and nonstationarities behavior [10].

Thus, in order to process magnetic Barkhausen noise and ultrasonic backscattering signal, a combined approach of detrended-fluctuation analysis (DFA) and principal component analysis (PCA) can be an interesting option. The variation of the detrended-fluctuations with size of the time window is a feature of the time series and this feature can be detected by pattern-classification tools. Principal component analysis can be used to obtain the maximum information in the initial data set so reducing their number of dimensions and simplifying the visualization of data. This approach was successfully used to study fault diagnosis from gearbox vibration signals [11].

The three nondestructive methods used to perform all inspections (ultrasonic testing, magnetic Barkhausen noise technique and eddy currents technique) are easy and fast. They can be used as complementary or alternative analysis to field metallography.

2. Methodology

UNS S31803 duplex stainless steel with composition shown in Table 1 was received as solution treated and contained only ferrite and austenite phases. Specimens with dimensions 300 mm × 300 mm × 10 mm were cut and machined. Specimens

Table 1
UNS S31803 alloy chemical composition (wt.%).

C	Mn	P	S	Si	Cr	Ni	Co
0.018	1.480	0.019	0.001	0.450	22.220	5.590	0.130
Cu	Mo	N	Nb	Al	Sn	Ce	Fe
0.280	3.080	0.180	0.021	0.003	0.012	0.020	66.496

were aged in two different temperatures (800 °C and 900 °C) for 5, 15, 30 and 120 min. Different sigma amounts were produced by this procedure. The specimens aged were compared to the as-received condition.

Each specimen was characterized by conventional methods: hardness and quantitative metallography for sigma phase percentage and percentage of ferrite using Ferristoscope®. Electrolytic etching with 10% KOH solution (3 V, 15 s) was used to reveal deleterious phases as dark regions in the micrographs. Quantitative metallography was performed with Image Tool, a freeware [12]. Light optical microscopy is unable to separate σ from χ phases and fine γ_2 . As explained, it was considered that the dark regions were only σ phase particles although it includes all deleterious phases mentioned.

The phase quantification results were used to evaluate the ones obtained from hardness and nondestructive tests namely ultrasound, eddy current and magnetic Barkhausen noise techniques. Brinell hardness tests were performed with a spherical indenter of 2.5 mm diameter and 187.5 kg load.

Both pulse-echo and backscattered signals were acquired during ultrasonic testing. The pulse-echo signals were used to calculate the velocity of sound through the samples from the wave transit time between two adjacent echoes. To perform the ultrasound tests, an ultrasound wave generator (Krautkramer, model USD15) was connected to a digital oscilloscope (Tektronix, model TDS3012B) and the signals were sent to a computer. Ultrasound transducers of 4, 5, 10 and 20 MHz were employed. Three pulse-echo signals and forty backscattered signals were acquired in random positions for all samples and for each frequency. The pulse-echo and backscattered signals were acquired with 10,000 (250 MSample/s) and 500 points (250 MSample/s), respectively.

Assuming that the sample thickness X is known (see Fig. 1a), the time-of-flight, τ_0 , between two adjacent echoes, $B_1(t)$ and $B_2(t + \tau_0)$ (see Fig. 1b), can be used to determine the group velocity of wave propagation through the media. The group velocity of propagation of the wave is given by

$$v = \frac{2X}{\tau_0} \quad (1)$$

The time-of-flight was estimated by the well-known cross-correlation method [6]. This method guarantees accurate velocity measurements. The values of τ_0 is computed as the value of τ for $-\infty \leq \tau \leq \infty$ for which

$$\left| \int_{-\infty}^{\infty} B_1(t) \cdot B_2(t - \tau) dt \right| \quad (2)$$

is maximum.

Putting down in words, the cross-correlation of two functions B_1 and B_2 involves shifting B_2 in τ toward B_1 and multiplying them in order to determine for which value of $\tau(\tau_0)$ this product is maximized. This means that the maximum of the integral of the cross-correlation between the echoes B_1 and B_2 , as a function of the time delay, corresponds to the situation where we have the best overlap of the echoes, i.e., they are at the situation of their maximum correlation.

For eddy current tests, a MIZ-21A ZETEC equipment and a 200 kHz probe were used. The probe was balanced (calibrated) in air and then placed on each sample surface. For each sample, three impedance measurements were made.

The experimental setup for magnetic inspection was basically a function generator, a power amplifier, a magnetic yoke, a coil pickup sensor and a data acquisition device. For the magnetic measurements, the yoke is placed on the sample surface so that the magnetic circuit is closed through the sample. The excitation is provided by a 10 Hz sine wave signal produced by a waveform generator and a bipolar power supply.

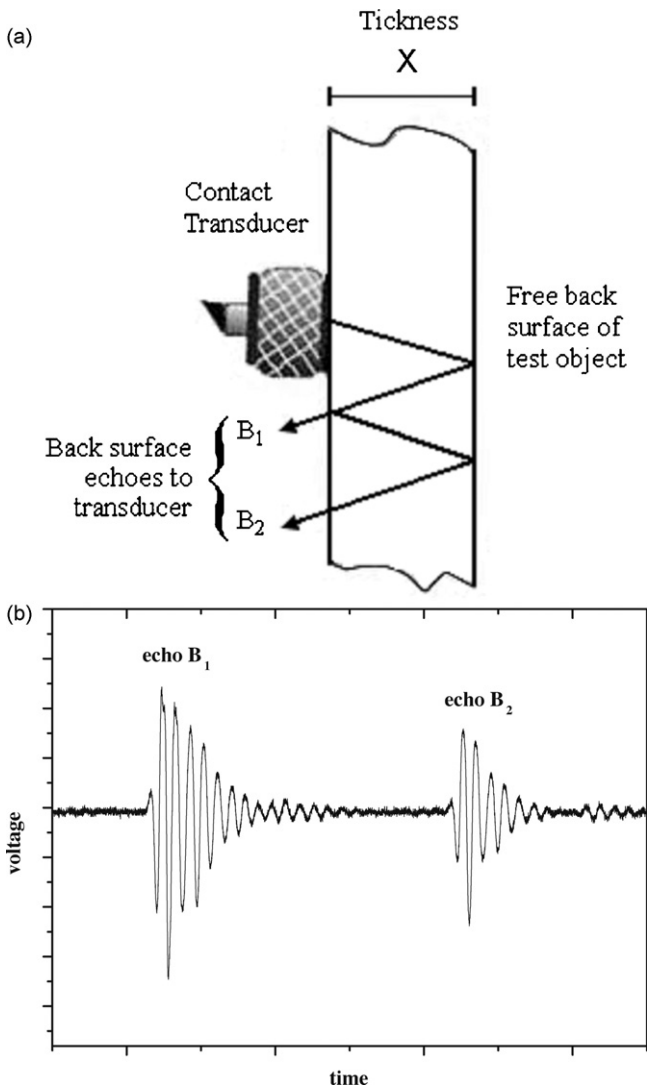


Fig. 1. (a) Diagram of an ultrasonic pulse-echo system for determining the velocity. (b) Time domain signal shows two successive back echoes acquired by pulse-echo method.

Two different kinds of signal were acquired during magnetic testing: magnetic Barkhausen noise (MBN) and flux density (B). The testing was carried out with a 10 Hz magnetization frequency and each signal was acquired with 40.000 points and 200 kSamples/s.

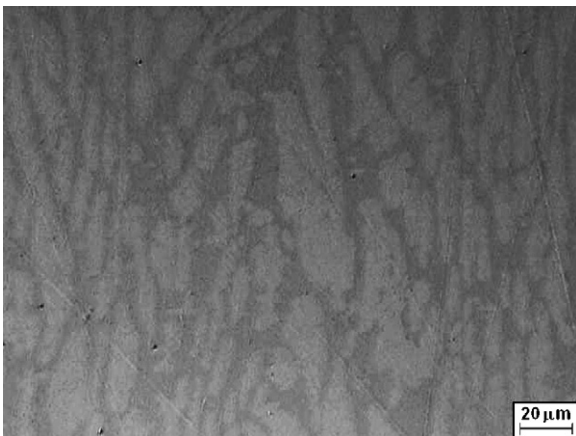


Fig. 2. Microstructure of solution treated specimen.

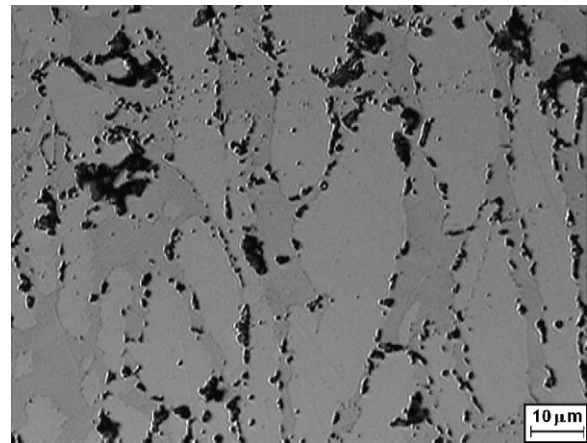


Fig. 3. Microstructure of specimen aged at 800 °C for 2 h.

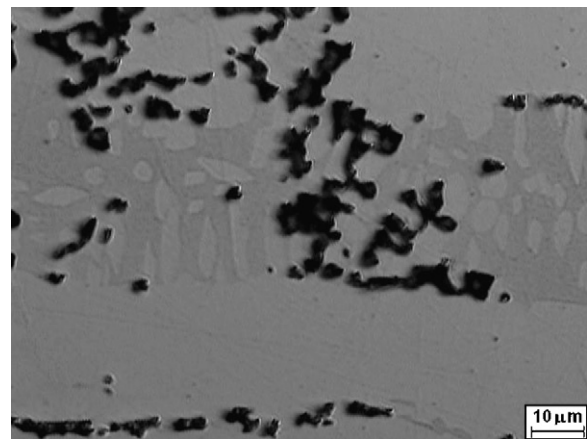


Fig. 4. Microstructure of specimen aged at 900 °C for 2 h.

Magnetic Barkhausen noise and ultrasonic backscatter signals were processed by the same combination of techniques to say DFA and PCA.

For each signal, DFA involved performing a linear fit to the data inside intervals of a certain size and evaluating the corresponding fluctuations detrended by the local fit. Repeating this procedure

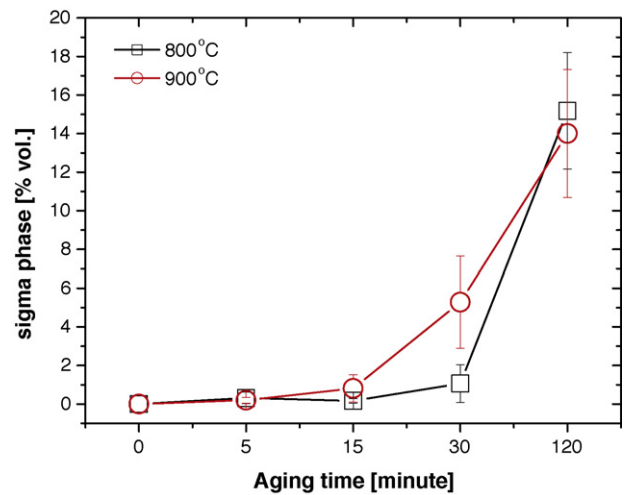


Fig. 5. Percentage of sigma phase from quantitative metallography as function of aging time at 800 °C and 900 °C.

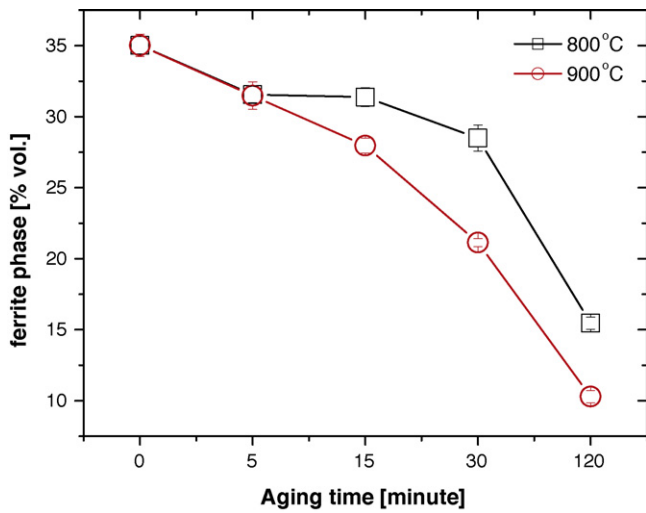


Fig. 6. Percentage of ferrite versus aging time at 800 °C and 900 °C.

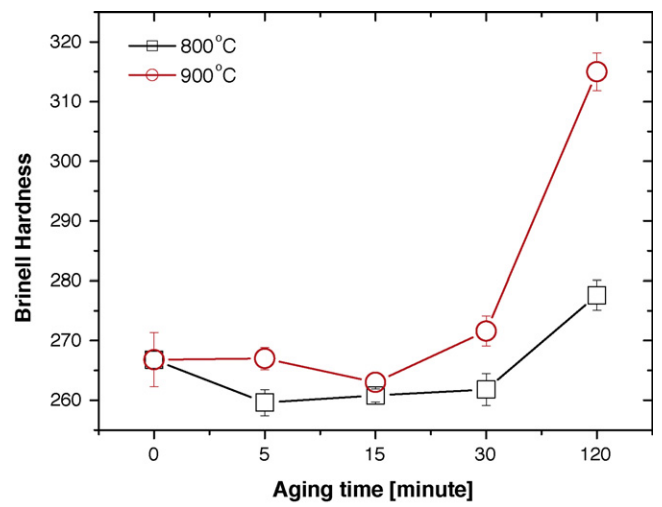


Fig. 7. Brinell hardness as function of aging time at 800 °C and 900 °C.

for many interval sizes yielded a plot of the average fluctuation as a function of size [10]. The variation of the detrended-fluctuations with the size of the time window is a feature of the time series and this feature can be captured by pattern-classification tools. Given a set of column vectors generated during detrended-fluctuation analysis, PCA was used to calculate the eigenvalues of the covariance matrix, sort the corresponding eigenvectors in decreasing order of the eigenvalues and rewrites the data vectors on the directions defined by those eigenvectors.

3. Results and discussion

Fig. 2 shows the microstructure of the solution treated specimen. Figs. 3 and 4 depict specimens aged at 800 °C and 900 °C for 2 h, respectively. Sigma phase is darkened by the etching while a soft contrast between ferrite and austenite phases is obtained. Sigma phase can be precisely quantified from these figures by image analysis. The micrographs also show that sigma phase forms at the expense of the ferrite phase.

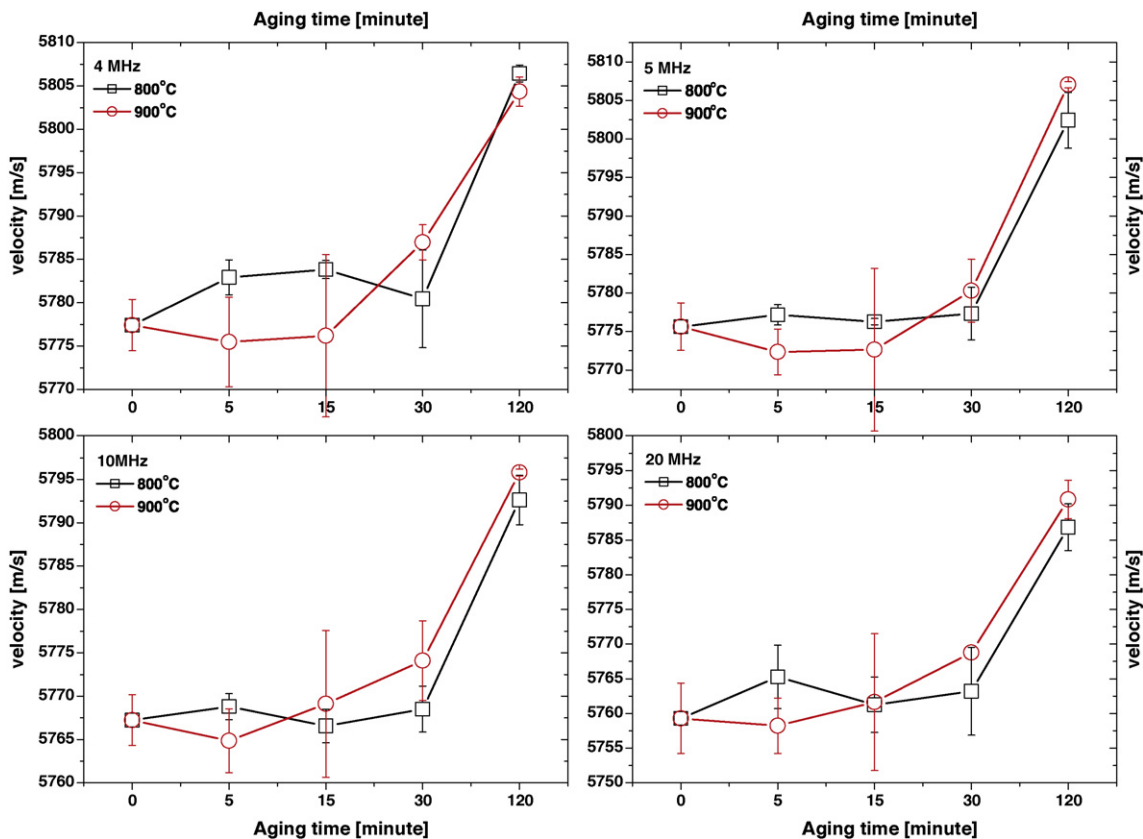


Fig. 8. Ultrasonic velocity of heat treated samples.

The results for percentage of sigma phase are presented in Fig. 5. The amount of ferrite phase measured with ferriscope as function of aging time is shown in Fig. 6. Brinell hardness measurements are shown in Fig. 7. Significant hardening is only detected after 5% volume fraction of sigma phase as observed by other authors [2,13].

The velocity of sound in each material is influenced by the density and the elastic moduli of the material [14]. Therefore, changes observed for the sound velocity indicate changes in material properties due to sigma phase generated from the ferrite phase. Ultrasonic velocity results show that it increases with time of heat treatment. This behavior was observed for all frequencies used, as shown in Fig. 8.

Eddy current testing provides a probe-specimen impedance measurement, which can be expressed as $Z = \sqrt{R^2 + X_L^2}$, where R and X_L are the resistance and inductive reactance components, respectively. Impedance is usually portrayed on an impedance-plane diagram, where the resistance component is plotted along one axis and the inductive reactance along the other axis.

Consequently, different values of resistivity and magnetic permeability result in characteristic coil impedance for each type of material, which correspond to particular points on the impedance-plane diagram.

If the eddy current circuit is calibrated in the absence of a sample and then brought near a conductive but nonferromagnetic material, some energy of the coil is used to generate eddy current in the material. The energy loss shows up as resistance component increasing. Furthermore, the magnetic field created by the eddy currents opposes the coil's magnetic field and the net effect is a weaker magnetic field to produce inductance. This is manifested as decrease of coil's inductive reactance.

A similar effect is observed in the resistance component for ferromagnetic materials. However, the coil magnetic field is concentrated in the sample due to its magnetic permeability. This increase in the magnetic field strength completely overshadows the magnetic field of the eddy currents. This appears as reactance increase on the impedance-plane diagram.

Thus, this method is sensitive to changes in electromagnetic properties of materials. Conversely, by measuring changes in resistance and inductive reactance of the coil, information, like changes in chemical composition, hardness, mechanical strength, and level of cold work, can be gathered about the test material. Therefore, this method is an indirect measure of overall physical and chemical properties.

In our measurements, when the coil was placed sequentially on a series of specimens, each with decreasing resistivity and permeability due to increasing of sigma phase fraction and decreasing of ferrite phase fraction, as shown in Figs. 5 and 6, respectively, a decrease in resistance and inductance reactance components is observed, resulting in impedance decreasing.

In this work, impedance-plane diagrams are not shown. Rather, impedance versus heat treatment conditions plots (Fig. 9) were constructed from eddy current measurement results. A very sharp decrease of impedance is observed in the first 15 min, which is not associated to sigma phase precipitation. This can be associated to some γ_2 precipitation and is also related to a very sharp softening detected in the same interval (see Fig. 7). An important decrease of impedance observed after 15 min is surely due to the paramagnetic sigma phase precipitation. In nonferromagnetic materials, the secondary electromagnetic field is derived exclusively from eddy currents. However, for ferromagnetic materials, additional magnetic effects usually overshadow the magnetic field generated by the induced eddy currents [5].

Figs. 10 and 11 show results obtained by a combined approach of detrended-fluctuation analysis (DFA) and principal component analysis (PCA) used to process ultrasonic backscattering signals and magnetic Barkhausen noise, respectively.

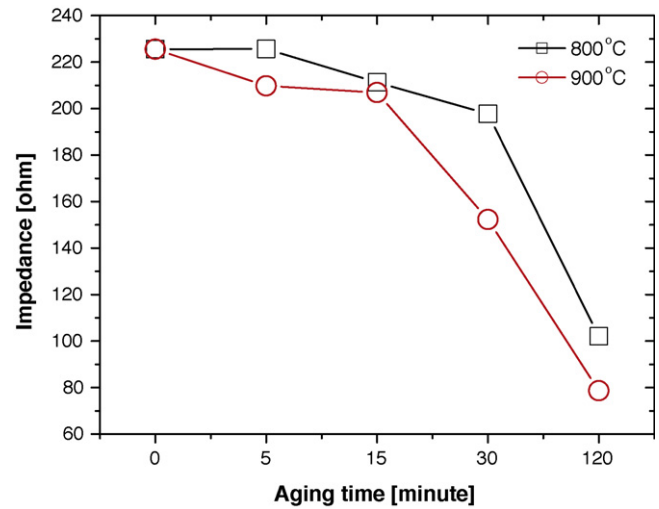


Fig. 9. Impedance versus heat treatment conditions.

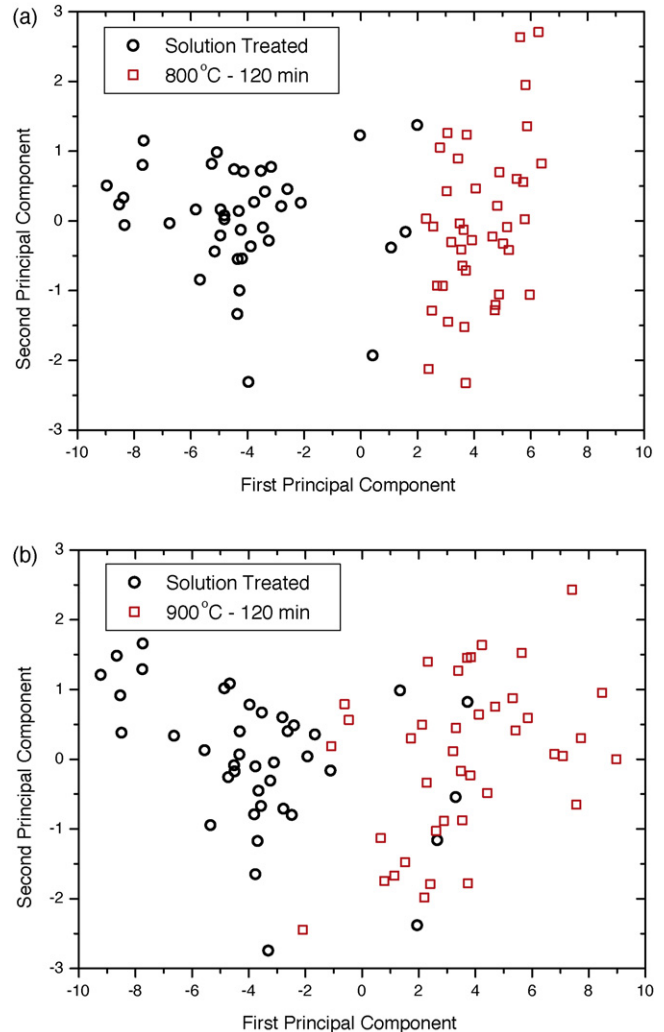


Fig. 10. (a) PCA applied to results produced using DFA from on backscattered signal acquired with 10 MHz for samples as-received and 800 °C for 120 min. (b) PCA applied to results produced using DFA from on backscattered signal acquired with 10 MHz for samples as-received and 900 °C for 120 min.

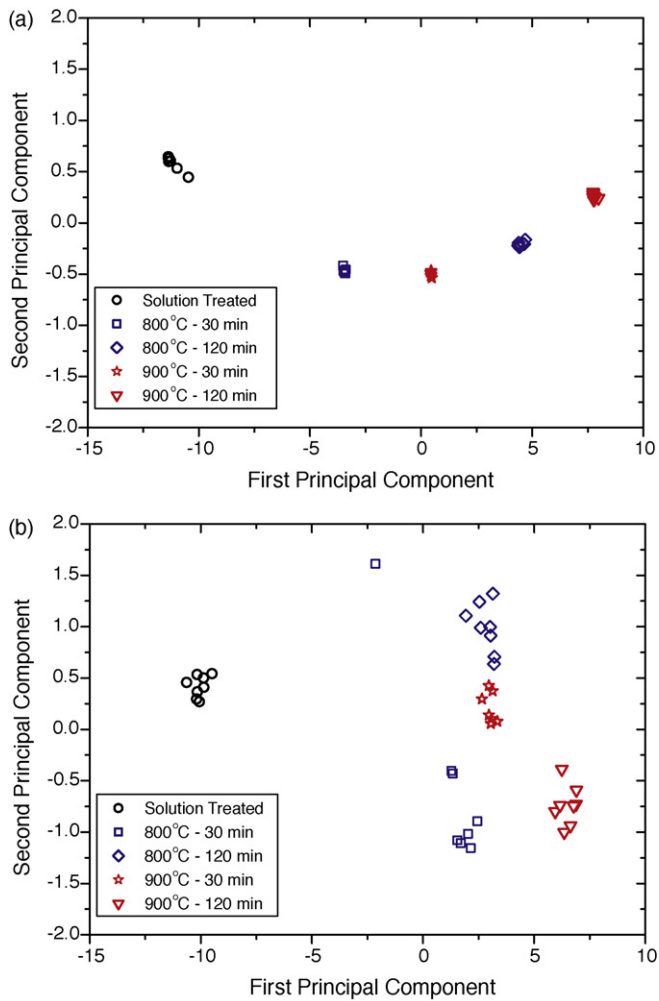


Fig. 11. (a) Principal component analysis applied to vector produced by detrended-fluctuation analysis from flux density signal acquired in different samples. (b) Principal component analysis applied to vector produced by detrended-fluctuation analysis from magnetic Barkhausen noise acquired in different samples.

Given a set of column vectors $\{\mathbf{x}_i\}$ generated during detrended-fluctuation analysis, PCA works by projecting the vectors onto the directions defined by the eigenvectors of the group-covariance matrix \mathbf{S} , defined as $\mathbf{S} = (1/N) \sum_{i=1}^N (\mathbf{x}_i - \mathbf{m})(\mathbf{x}_i - \mathbf{m})^T$ in which \mathbf{m} is the average vector, $\mathbf{m} = (1/N) \sum_{i=1}^N \mathbf{x}_i$ and \mathbf{T} denotes the vector transpose [9]. The projection along the direction of the eigenvector corresponding to the largest eigenvalue of \mathbf{S} is the first principal component, and accounts for the largest amount of variation in the original vectors. The remaining principal components are arranged in decreasing order of the corresponding eigenvalues. It follows that the projection on the second largest eigenvector related to the second largest eigenvalue gives the second principal component [9].

Fig. 10 shows plots of the second versus the first principal components calculated from the DFA results obtained from ultrasonic

backscattered signals acquired in specimens heat treated in different temperature.

Fig. 11 shows results obtained by the same sequence of processing as Fig. 10, but now for magnetic Barkhausen noise acquired in five specimens submitted to different temperature and aging time.

It should be noticed that this combined approach was able to recognize patterns and discriminate between signals obtained from different heat treatment conditions.

It is follows that the processing of flux density signal show better performance than using magnetic Barkhausen noise in the classification of the studied classes.

4. Conclusion

It was demonstrated that it is possible to monitor phase transformations and specifically sigma generation on a UNS S31803 duplex stainless steel based solely on nondestructive testing.

The sigma phase formation causes changes in magnetic and mechanical properties material. Impedance and ultrasonic velocity measurements are sensitive to these changes and can be used to detect this transformation.

Furthermore, the combination of techniques used to process backscattered signals and magnetic Barkhausen noise was able to distinguish between signals acquired from sample with different phase sigma percentage.

These techniques were shown to be promising methods for sigma phase monitoring.

Acknowledgements

The authors acknowledge financial support from the Brazilian agencies FUNCAP, CNPq, CAPES and UFC. Elineudo P. Moura acknowledges fruitful discussion with Prof. Lindberg L. Gonçalves.

References

- [1] R.N. Gunn, Duplex Stainless Steels—Microstructure, Properties and Applications, Abington Publishing, Cambridge, 2003.
- [2] J.O. Nilsson, Materials Science and Technology 9 (1992) 685–700.
- [3] M. Pohl, O. Storz, T. Glogowski, International Journal of Materials Research 10 (2008) 1163–1170.
- [4] S.K. Gosh, S. Mondal, Materials Characterization 59 (2008) 1776–1783.
- [5] ASM Handbook, Nondestructive Evaluation and Quality Control, vol. 17, 9th ed., The Materials Information Society, New York, 1989.
- [6] Nondestructive Testing Handbook, Ultrasonic Testing, vol. 7, 2nd ed., ASTM, New York, 1991.
- [7] A.Y. Kina, S.S.M. Tavares, V.M. Souza, L.D. Lima, R.R.A. Corte, J.M. Pardal, Materials Characterization 59 (2008) 1127–1132.
- [8] C. Chatfield, The Analysis of Time Series, 5th ed., Chapman & Hall/CRC, Boca Raton, 1996.
- [9] A.R. Webb, Statistical Pattern Recognition, 2nd ed., John Wiley & Sons, West Sussex, 2002.
- [10] Z. Chen, P.Ch. Ivanov, K.un. Hu, H.E. Stanley, Physical Review E 65 (2002) 1–15.
- [11] E.P. Moura, A.P. Vieira, M.A.S. Irmão, A.A. Silva, Mechanical Systems and Signal Processing 23 (2009) 682–689.
- [12] Image Tool version 3.0, University of Texas Health Science Center at San Antonio, 2002, free software, available in the website <http://ddsdx.uthscsa.edu/dig/itdesc.html>.
- [13] T.H. Chen, K.L. Weng, J.R. Yang, Materials Science and Engineering A 338 (2002) 259–270.
- [14] P.J. Shull, Nondestructive Evaluation—Theory, Techniques and Applications, Marcel Dekker, New York, 2002.